Published in final edited form as:
Gene Ther. 2010 July ; 17(7): 815–826. doi:10.1038/gt.2010.29.

Self-complementary AAV-mediated gene therapy restores cone function and prevents cone degeneration in two models of Rpe65 deficiency

Jijing Pang[1a,*], **Shannon E. Boye**[1a,*], **Bo Lei**[2,3], **Sanford L. Boye**[1a], **Drew Everhart**[4], **Renee Ryals**[1a], **Yumiko Umino**[4], **Bärbel Rohrer**[5], **John Alexander**[1b], **Jie Li**[1a], **Xufeng Dai**[6,1a], **Qiuhong Li**[1a], **Bo Chang**[7], **Robert Barlow**[4], and **William W. Hauswirth**[1a]

[1a] Department of Ophthalmology and Powell Gene Therapy Center, University of Florida, Gainesville, FL 32610

[1b] Molecular Genetics & Microbiology, University of Florida, Gainesville, FL 32610

[2] Veterinary Medicine and Surgery, Ophthalmology, University of Missouri, Columbia, MO 65211

[3] Ophthalmology, the First Affiliated Hospital of Chongqing Medical University, Chongqing Key Laboratory of Ophthalmology, Chongqing, 400016, China

[4] Ophthalmology, SUNY Upstate Medical University, Syracuse, NY 13210

[5] Departments of Ophthalmology, and Neurosciences Division of Research, Medical University of South Carolina, Charleston, SC 29425

[6] Eye Hospital, School of Optometry & Ophthalmology, Wenzhou Medical College, Wenzhou, China 325027

[7] The Jackson Laboratory, Bar Harbor, ME 04609

Summary

To test whether fast-acting, self complimentary(sc), AAV vector-mediated RPE65 expression prevents cone degeneration and/or restores cone function, two mouse lines were studied: the *Rpe65*- deficient *rd12* mouse and the *Rpe65*- deficient, rhodpsin null ('i.e. cone function-only') *Rpe65*$^{-/-}$::*Rho*$^{-/-}$ mouse. scAAV5 expressing RPE65 was injected subretinally into one eye of *rd12* and *Rpe65*$^{-/-}$::*Rho*$^{-/-}$ mice at postnatal day 14 (P14). Contralateral *rd12* eyes were injected later, at P35. *Rd12* behavioral testing revealed that rod vision loss was prevented with either P14 or P35 treatment, while cone vision was only detected following P14 treatment. Consistent with this observation, P35 treatment only restored rod ERG signals, a result likely due to reduced cone densities at this time point. For *Rpe65*$^{-/-}$::*Rho*$^{-/-}$ mice in which there is no confounding rod contribution to the ERG signal, cone cells and cone-mediated ERGs were also maintained with treatment at P14. This work establishes that a self-complimentary AAV5 vector can restore substantial visual function in two genetically distinct models of Rpe65- deficiency within 4 days of treatment. Additionally, this therapy prevents cone degeneration but only if administered prior to extensive cone degeneration, thus supporting continuation of current LCA2 clinical trials with an added emphasis on cone subtype analysis and early intervention.

Address Correspondence to: Ji-jing Pang, M.D., Ph. D. Department of Ophthalmology, College of Medicine, University of Florida 1600 SW Archer Road, Gainesville, FL 32610 Tel: 352-392-0471; Fax: 352-392-0573; jpang@ufl.edu.
*These authors contributed equally to the development of this manuscript

Keywords

Leber's congenital amaurosis-2 (LCA2); RPE65; Adeno-associated virus (AAV); retinal gene therapy; *rd12* mice; *Rpe65*$^{-/-}$::*Rho*$^{-/-}$ mice

INTRODUCTION

Leber's congenital amaurosis-2 (LCA2), one of the earliest and most severe forms of inherited retinal dystrophies[1], has been linked to mutations in *Rpe65*, a gene whose protein product, RPE65 (retinal pigment epithelium specific 65 kDa protein) plays a crucial role in the visual cycle. It restores light sensitivity to the retina by enzymatically converting the all-trans isomer to its light active 11-cis form. While much is known about the retinoid cycle and RPE65 as it pertains to rod photoreceptors, less is known about its role in cones. However, recent studies suggest a clear dependency of cones on this isomerase activity [2–5], and LCA2 patients exhibit early foveal cone loss [6]. Importantly, these patients retain some foveal cones for decades, leading to the idea that this may be the result of a supplemental cone-specific retinoid recycling pathway.[7,8,9,10] Understanding the relationship between RPE65 and cone photoreceptors is all the more important because cones are responsible for the perception of images in bright light, colors and fine visual details.

Recently, early results of several phase I or I/II LCA2 clinical trials[11–15] reported a lack of short-term safety concerns (up to one year) and modest increases in visual function in young adult patients receiving AAV-mediated gene replacement therapy. By using chromatic stimuli and light adaptation conditions, Cideciyan et al.[14] were able to isolate both rod and cone photoreceptor contributions to the enhanced visual sensitivity in the retinas of treated patients. It is important to note that treated retinal areas in LCA2 patients do not contain a normal compliment of retinal cells and that these areas may be susceptible to further cell loss due to negative bystander effects from untreated, neighboring degenerate retina[16]. Additionally, it has been reported that under conditions of limited chromophore supply, rods and cones compete for RPE65-regenerated 11-cis-retinal[17]. These facts highlight the potential advantages of early intervention and the targeting of retinal islands which contain the maximum compliment of remaining cone photoreceptors.

In spite of the encouraging Phase I/II clinical results, important questions remain to be answered regarding AAV-mediated *Rpe65* gene therapy. Is gene therapy alone capable of preventing cone photoreceptor degeneration? What is the therapeutic window? How does the presence or absence of rod photoreceptors in treated retinal areas affect the ability of AAV-Rpe65 to restore function to and/or prevent degeneration of cone photoreceptors? Lastly, does gene therapy result in sufficient restoration of rod and cone function detectable by an objective functional assay such as ERG? These questions are best initially addressed in animal models of the disease for several reasons: First, the currently reported clinical trials evaluated AAV-*Rpe65* therapy in young adults or older children whose retinas had already exhibited extensive degeneration[11–15]. Second, there are no technologies routinely available to precisely quantify cone photoreceptor densities distant from the fovea *in-vivo*, although this may change in the near future[18]. Currently, only post-mortem microscopic examination of treated eyes would allow for such quantification. The question of how the presence of rod photoreceptors affects therapeutic efficiency in cones is more easily ascertained in Rpe65-deficient animal models because, unlike in LCA2 patients, we have a more complete understanding of the temporal and spatial degeneration patterns of both photoreceptor subtypes. Lastly, retinal function, as assessed by full-field ERG is not a sensitive measure of efficacy in treated LCA2 patients due to the relatively small area of retina often transduced with therapeutic vector and the limited fraction of photoreceptors

remaining for functional rescue. Multifocal ERG might be useful in this regard, but again, all of these issues can be addressed more directly in animal models of LCA2.

The purpose of this study was to test whether early versus late delivery of RPE65 would confer functional rescue to cone photoreceptors and or prevent their degeneration in two *Rpe65*-deficient animal models, the *rd12* mouse and the *Rpe65*$^{-/-}$::*Rho*$^{-/-}$ double knockout (DKO) mouse. Studies have shown that true cone-mediated responses in *Rpe65*- deficient mice are masked by rods with elevated thresholds and altered response kinetics[19]. This provides the rationale for evaluating therapy in the *Rpe65*$^{-/-}$::*Rho*$^{-/-}$ mouse, a model which lacks functional rhodopsin, rod outer segments and any rod-mediated light response. This DKO mouse allowed for assessment of pure cone function upon Rpe65 gene therapy in the absence of interference from rod-mediated responses[19]. Early intervention was achieved with the use of a quick onset, self-complimentary AAV vector[20–23] containing human RPE65 cDNA (scAAV5-smCBA-hRPE65). Electroretinogram (ERG), visually-evoked behavioral tests and cone-specific immunostaining were used to determine levels of cone preservation upon early (P14) and late (P35) vector treatment in the *rd12* mouse. The effects of P14 treatment on pure cone function and structure were also evaluated in the *Rpe65*$^{-/-}$::*Rho*$^{-/-}$ mouse. Cone loss due to the bystander effects of rod loss[24, 25] in the *Rpe65*−/−::*Rho*−/− mouse rendered analysis of P35 treatment impossible. Our results show that AAV-mediated gene therapy can restore function to cones and prevent early cone degeneration but only if therapy is initiated prior to extensive retinal degeneration. Additionally, this study suggests that therapy may prove maximally beneficial to cone photoreceptors when it is targeted to retinal islands containing mostly cones and few rods. Our results also show that early intervention, using a self-complimentary AAV5 vector restores substantial visual function within 4 days following treatment. Because progressive cone loss is associated with visual acuity deficits in LCA2 patients, gene therapy may have its greatest impact in young retinas before such cone loss occurs.

RESULTS

Therapy in the *rd12* mouse

Cone photoreceptor densities are normal in untreated P14 *rd12* mice but decrease progressively and in a geographically specific manner—Cone photoreceptor densities in *rd12* and *C57BL/6J* mice were analyzed by staining with peanut agglutinin (PNA), a lectin that selectively labels the interphotoreceptor matrix associated with cone photoreceptors in a variety of species. Comparisons of cone cell counts in PNA-stained retinal wholemounts revealed that there was no significant difference in cone photoreceptor densities between any region of P14 *rd12* and P14 WT mice (Fig 1a, c, Table 2, Supplemental Table 1). Cones are abundant throughout the peripheral and central (Fig 1b, d) retinas of both strains at this time point. The black areas in the central retina of P14 *rd12* mice (Fig 1d) are fragments of adherent retinal pigment epithelium, a layer sometimes difficult to dissociate from neural retina in young *rd12* mice. By 5 weeks of age, cone densities have significantly decreased relative to P14, with only a fraction of cones remaining in the dorsal and temporal retina (Fig 1e, Table 2, Supplemental Table 1). At 5 months, this cone loss now encompassed the entire inferior hemisphere (Fig 1f), with the remaining cones positive only for M-cone opsin (data not shown).

Rod-mediated ERG is preserved with either P14 or P35 treatment but cone-mediated ERG is only preserved with P14 treatment in *rd12* mice—In *rd12* eyes treated with scAAV5-smCBA-hRPE65 at P14, restored dark-adapted ERGs were detected as early as 4 days after treatment (Fig 2a). Both dark- and light-adapted ERGs in animals treated at P14 became stable in amplitude around 2 weeks post-treatment (data not shown)

and remained so for at least 6 months (the latest time assessed following treatment, Fig 2b, d). Restoration of dark-adapted ERGs was observed in both early P14 (n=5) and late P35 (n=5) treated eyes (Fig 2b, c). The average b-wave amplitudes at 0.65 log cd-s/m^2 intensity were 382.38±26.21 (n=4), 293.86 ±103.80 (n=6) and 263.04 ±81.25 (n=6) in normal C57 BL/6J, P14 treated and P35 treated eyes, respectively. The b-wave amplitudes in P14 and P35 treated *rd12* eyes were about 76% and 68% of those from uninjected, isogenic normal mice. There was no significant difference between P14 and P35 treatments for both a-wave (P=0.6688) and b-wave (P=0.1661) amplitudes.

Although dark-adapted ERG responses remained stable and a- and b-wave amplitudes were approximately equivalent in both P14 and P35 treated eyes (Fig 2b), there was a distinct difference between the restoration of light-adapted ERGs in P14 vs. P35-treated eyes in the same *rd12* animal (Fig 2d, e, f). With the highest stimulus light intensity (0.65 Log cd-s/m^2), amplitudes of cone-driven ERG b-waves in P14-treated eyes were significantly restored compared with untreated age-matched *rd12* eyes (52.51 ± 13.53 μV vs. 13.00 ± 4.72 μV, P = 0.009), whereas only minimal ERG responses were recorded in the P35-treated eyes (20.73 ± 3.77μV vs. 13.00 ± 4.72 μV, P = 0.252). Cone b-wave amplitudes of P14-treated eyes (52.51 ± 13.53 μV) were about 60% of normal *C57BL/6J* mice (87.28 ± 13.06 μV, P = 0.0359) and were significantly larger than those of P35-treated *rd12* eyes (20.73 ± 3.77μV, P = 0.0293).

To test whether early- and late-treatments affected the sensitivity of the cone system, we measured the implicit time of the cone driven b-wave. Interestingly, implicit times for the P14-and P35-treated *rd12* groups were similar (45.84 ± 1.22 ms vs. 49.52 ± 2.99 ms, P = 0.166), and both showed no difference when compared to the normal *C57BL/6J* controls (49.80 ± 1.92 ms, P = 0.071 and P = 0.902, respectively). Both P14- and P35-treatments corrected the delayed implicit time of the cone-driven responses in the *rd12* mice (64.00 ± 4.18 ms, P = 0.001 and P =0.007, respectively).

To further validate rescue of rod- and cone-mediated responses in vector treated *rd12* eyes, we recorded 10 Hz flicker ERG responses in darkness (Fig 2h)[19]. The amplitude-intensity curve of such a recording protocol presents two peaks which represent the rod- and cone-driven responses respectively (Fig 2i). Five months after treatment, rod-mediated function was restored in both P14- and P35-treated *rd12* eyes and the response amplitudes were similar. In contrast, major cone-mediated responses were restored only in P14-treated eyes (Fig 2h, i). These results were consistent with those generated with conventional, single stimulus ERG recordings.

Optomotor behavior reveals the efficacy of scAAV-RPE65 for rescue of both photopic and scotopic vision in the *rd12* mouse with P14 treatment, but only scotopic vision with P35 treatment—Optomotor analysis showed that wild type mice (Fig. 3, white bars, n=4) responded significantly better than *rd12* untreated eyes (black bars, n=3) under all conditions. Under scotopic conditions (Figure 3a, 3b), untreated *rd12* eyes function poorly with an acuity of 0.079 ± 0.013 cyc/deg (Figure 3a, black bar, mean + SD, n=3). *C57BL/6J* control eyes respond significantly better, displaying an acuity of 0.355 ± 0.039 cyc/deg (white bar, n=4). *Rd12* eyes vector treated at P14 have an acuity of 0.370 ± 0.031 cyc/deg (light grey bar, n=4), a level essentially identical to wild type eyes and significantly better than untreated *rd12* control eyes ($p < 0.0001$). Eyes treated at P35 responded like C57BL/6J eyes under dark-adapted conditions, with an acuity of 0.390 ± 0.080 cyc/deg (dark grey bar, n=3), and significantly better than their untreated control eyes (black bar, 0.079 ± 0.013, n=3, P=0.0026). Statistical comparisons of these measurements are shown in Table 1.

Scotopic contrast sensitivities (Figure 3b) paralleled the scotopic acuity results, with eyes treated at P14 (contrast sensitivity of 3.97 ± 0.35, n=4), and eyes treated at P35 (contrast sensitivity of 4.78 ±0.49, n=3) showing contrast thresholds nearly identical to wild type mice (4.40 ± 0.74, n=4). Again, *rd12* eyes treated at P14 and P35 performed significantly better than *rd12* untreated eyes, which display a contrast sensitivity of 1.05 ± 0.03 (n=3, $p<0.0001$ for both comparisons). In all scotopic tests, untreated *rd12* eyes perform extremely poorly, essentially equivalent to no rod-mediated visual function.

Under photopic, cone-dominated conditions, *C57BL/6J* wild type control eyes functioned well, displaying an average acuity of 0.499 ± 0.39 cyc/deg (Figure 3c, white bar, n=4) and average contrast sensitivity of 8.79 ± 2.79 (Figure 3d, white bar, n=4). As with scotopic conditions, untreated *rd12* mice exhibited significantly poorer visual acuities and contrast sensitivities than wild type *C57BL/6J* controls, however, untreated *rd12* eyes still exhibit measurable acuities under photopic conditions, a result likely due to the contribution of desensitized rods[20] to visual behavior. Treatment of *rd12* eyes at P14 improves acuity (0.481 ± 0.040 cyc/deg, n=4, $p = 0.0091$) and contrast sensitivity (9.19 ± 6.93, n=4, $p=0.022$) compared to untreated *rd12* eyes (acuity = 0.333 ± 0.055 cyc/deg and contrast sensitivity of 2.34 ± 0.53, n=3 each). Treatment at P35 had no statistically significant impact on cone-mediated acuity or contrast sensitivity.

Treatment of *rd12* mice at P14 but not at P35 prevents cone degeneration— Five months after the second eye subretinal injection of AAV5-sc-smCBA-hRPE65 vector at P35, *rd12* cone densities and opsin profiles were analyzed with PNA, M-cone opsin and S-cone opsin antibody staining. By comparing the number of cone photoreceptors stained with either PNA, MWL or SWL cone opsin, we found no significant differences between cone photoreceptor densities in the four quadrants of P14-treated *rd12* and P14 WT retinas (Fig. 4a–d, Table 2, Supplemental Table 2a). In contrast, P35- treated eyes showed significant cone loss relative to P14-treated eyes, again with the exception of the dorsal and temporal quadrants (Fig 4e–h, Table 2, Supplemental Tables 2a, 2b). There were no significant differences in cone densities between P35-treated and untreated *rd12* eyes at 5 months (Fig 4e–h, Table 2, Supplemental Table 2a). Residual cones in P35-treated *rd12* retinas stained positive for M-cone but not S-cone opsin (Fig 4g, h).

Therapy in the *Rpe65*$^{-/-}$*::Rho*$^{-/-}$ mouse

Cone photoreceptor densities are normal in untreated P14 but not untreated P35 *Rpe65*$^{-/-}$::Rho$^{-/-}$ mice—PNA-staining of retinal wholemounts revealed that there was no significant difference in cone photoreceptor densities in any quadrant of untreated P14 *Rpe65*$^{-/-}$::*Rho*$^{-/-}$ and P14 wild type mice (Fig 5a and b, Fig 1a, Table 2, Supplemental Table 3a). Cones appear throughout the peripheral and central retinas at this age. By five weeks, cone densities have significantly decreased relative to P14 *Rpe65*$^{-/-}$::*Rho*$^{-/-}$ mice, (Fig 5c, Table 2, Supplemental Table 3a) with only a few cones remaining in the dorsal and temporal regions of the retina (Fig 5c), a pattern similar to that observed in the untreated, P35 *rd12* mouse (Fig 1e).

Cone photoreceptors and cone-mediated ERG are preserved with P14 vector treatment of Rpe65$^{-/-}$::Rho$^{-/-}$ mice—In *Rpe65*$^{-/-}$*::Rho*$^{-/-}$ eyes treated with rAAV5-sc-smCBA-hRPE65 at P14, dark-adapted (rod-mediated) ERGs were undetectable (data not shown). This was expected due to the absence of rhodopsin in this animal. Light-adapted (cone-mediated) responses were detectable as early as 4 days post-treatment (Fig 6a). These responses became stable in amplitude (data not shown) and remained at this level for at least six weeks. At six weeks (the latest time point evaluated), at the highest stimulus intensity (1.4 log cd-s/m^2), the amplitudes of cone-driven ERG b-waves in P14-treated eyes

were significantly restored relative to the untreated, contralateral *Rpe65*$^{-/-}$*::Rho*$^{-/-}$ eyes (99.01 ± 16.17 mV vs. 2.30 ±2.02 mV, P= 0.0001) (Fig 6b, 6c). Restored, light-adapted amplitudes were approximately 60% of those from Rho$^{-/-}$ mice with normal RPE65 genes at a similar age[25]. Approximately 4 weeks following vector injection, PNA-based cone counts revealed no significant difference in cone photoreceptor densities between the four quadrants of P14-treated *Rpe65*$^{-/-}$*::Rho*$^{-/-}$ and P14 WT mice (Fig 7a, 7b, Table 2, Supplemental Table 3a). M-cone opsin and S-cone opsin antibody staining revealed that both pigments were present in preserved cones (Fig 7c, 7d, Table 2, Supplemental Table 3b). Thus P14-treatment both prevents cone loss and preserves cone-mediated function in a second model of RPE65-mediated photoreceptor degeneration.

DISCUSSION

Documentation of cone loss in *rd12* retinas with PNA lectin revealed that the optimal treatment age in this model is P14. At this age, cone densities remained near normal in both central and peripheral retina. Cone degeneration became obvious in rd12 mice older than 3 weeks. By P35, significant cone loss had occurred in untreated *rd12* eyes, an observation similar to that seen in other Rpe65-deficient models[2, 27, 28]. Here we show that early (P14) treatment of *rd12* mice with a quick-onset, self complimentary (scAAV) vector containing the human *Rpe65* cDNA restores ERG responses and visually evoked behavior to both rod and cone photoreceptors and prevents both MWL- and SWL-containing cone degenerations for at least 6 months. These results are consistent with and extend previous findings that both lentiviral- and adenoviral-mediated RPE65 expression confers rescue to cones in the Rpe65$^{-/-}$ mouse which carries a different, null mutation[29,30]. Recovered light-adapted responses imply restoration of cone pigment kinetics. While the precise kinetics of cone adaptation by ERG was not studied in the current work, it would be of interest because it may represent another useful parameter of cone health after gene therapy. In contrast, treatment delayed by just 3 weeks still rescued rods functionally and by acuity/contrast sensitivity, a result not seen for cones.

This is one of the first studies to demonstrate the advantages of scAAV over classic AAV vectors in terms of its ability to restore function more rapidly in a retinal degenerative model while further confirming earlier reports of its ability to elicit more rapid transgene expression[20–23]. Like classic serotype 5 AAV, scAAV5-mediated transgene expression is not limited to the RPE. Regardless, we observed therapeutic transgene expression mainly located within RPE cells[23], the key cellular target for rod and cone rescue. When using standard AAV vectors, it is typically necessary to wait one month post-injection to evaluate therapeutic efficacy. Bearing in mind that, in terms of biological time, one month of a mouse's life corresponds to approximately several years of human life, these results have important implications for ongoing LCA2 clinical trials by suggesting that early intervention may increase the chance of preserving cone photoreceptors and restoring cone function to these patients[31]. However, precisely how this short window of therapeutic response in mice relates to the human condition remains to be determined.

The possibility that desensitized rods may have contributed to the ERG and behavioral results we attributed to rescued cone function in P14 vector-treated *rd12* mice is not supported by analysis of analogous treatment in "cone-function-only" *Rpe65*$^{-/-}$*::Rho*$^{-/-}$ double knockout mice. Since rods in this animal lack rhodopsin, there can be no rod phototransduction and hence no rod source of light-elicited electrical activity to confound ERG analysis. Although this experiment is similar to a study in which lentiviral-mediated *Rpe65* therapy was administered to the Rpe65$^{-/-}$/Gnat1a$^{-/-}$ mice which also lack rod function due to a mutation in rod transducin[29], our study utilizes AAV, a well characterized viral vector with documented clinical safety in the retina[11–15] and with different tropism and

transduction characteristics than lentivirus. We observe cone rescue at all levels of analysis with P14 treatment of the *Rpe65*$^{-/-}$*::Rho*$^{-/-}$ mouse for at least four weeks post-treatment. Self-complimentary vector conferred ERG rescue as early as 4 days post-treatment. However, attempts to prevent cone degeneration and/or confer function to cones in late-treated *Rpe65*$^{-/-}$*::Rho*$^{-/-}$ mice were unsuccessful (data not shown). The inability to reexamine the question of a window of therapy in the *Rpe65*$^{-/-}$*::Rho*$^{-/-}$ mouse was likely due to the fact that cones in this double knockout model have extensively degenerated prior to one month of age[2]. In addition, rods in rhodopsin-deficient mice begin to degenerate within one month of life[32,33], which leads to cone degeneration at least partially through reduction in a rod-derived cone viability factor, RdCVF[25]. Thus, cone and rod degeneration and perhaps other structural or biochemical abnormalities that accompany early photoreceptor cell death[34–36] preclude analysis of late (P35) AAV vector-mediated cone therapy in *Rpe65*$^{-/-}$*::Rho*$^{-/-}$ mice. Nevertheless, cone rescue as seen in the P14-treated *rd12* model was confirmed in a retina having only cone function.

Our results are consistent with earlier findings that cone cell death in *Rpe65*-deficient animal models proceeds in a rapid, cone subtype-dependent manner; SWL-cones degenerating faster than MWL- cones[2,27,28]. In support, analysis of LCA2 patients also reported differences in chromatic sensitivities between long and short-wavelength light: only human LWL-cone function was detectable in LCA2 patients carrying various *Rpe65*-mutations, SWL-cone function being undetectable[5]. Despite the fact that murine retinas lack true LWL-cones, it is worth noting that SWL cones still appear to be the most sensitive to *Rpe65*-deficiency across species. In another study, it was shown that cone opsin mislocalization in the *Rpe65*$^{-/-}$*::Rho*$^{-/-}$ was corrected with systemic administration of 11-cis retinal[2]. This correction was more pronounced in MWL cones than in SWL cones. The reasons that SWL-cones appear to be more adversely affected by chromophore depletion remain to be elucidated. It is possible that type-specific differences in opsin stability in the absence of chromophore could play a role in cone survival. It is known, for example, that glycosylation is not required for the formation of functional bovine MWL cone pigment[37] suggesting that there are intrinsic structural differences between MWL and SWL opsins despite their amino acid sequence similarities. Perhaps MWL cone opsin in the absence of 11-cis retinal is slightly more stable than SWL opsin leading to a slower rate of accumulation of misfolded MWL opsin aggregates and a slower rate of MWL cone cell death. Here we show that AAV-RPE65 therapy is capable of preserving both cone photoreceptor subtypes as long as therapy is initiated prior to extensive cone degeneration. The differential ability of this therapy to preserve one cone subtype over another, although not yet evaluated in LCA2 patients[11–15], deserves further examination.

In order to compare overall functional differences (ERG and optomotor) following P14 and P35 treatment in eyes that had received comparable vector coverage of their retinas, we only chose *rd12* mice in which both eyes exhibited similar levels of retinal detachment following subretinal vector injection. This method for selecting equivalently treated pairs of partner eyes is validated by the similar rod-related ERG amplitudes seen in both P14 and P35 treated eyes (Figure 2b). Mice used in this study had 60–-80% retinal detachments in both eyes post-injection, and this level of vector treatment corresponds well to the level of ERG restoration seen (Figure 4e). Experiments are ongoing to test whether MWL cone function can be restored following P35 treatment when that small dorsal area of remaining MWL cones is specifically targeted by vector injection.

While ERG recordings in the *rd12* and *Rpe65*$^{-/-}$*::Rho*$^{-/-}$ mice cannot be directly compared because they were done at different institutions, we believe it is interesting to note that cone-mediated ERG responses in *Rpe65*$^{-/-}$*::Rho*$^{-/-}$ mice were higher than responses in *rd12* mice at the same stimulus intensity (0.7 log cds/m^2). This result is consistent with a recent

finding that under conditions of limited chromophore supply, rods and cones compete for RPE65-regenerated 11-cis-retinal[17]. Rods, due to their higher number, proximity to the RPE as a chromophore source and the instability of cone opsins relative to rhodopsin, are likely privileged under this condition. Interestingly, it is specifically the absence of rhodopsin (and not simply the absence of rod outer segments) which allows cones to benefit from the availability of more 11-cis-retinal. It is understandable, therefore, that we observed a difference in cone-mediated responses between these two animal models. Put simply, both rods and cones compete for gene therapy-derived chromophore in the *rd12* mouse, whereas in the *Rpe65*$^{-/-}$*::Rho*$^{-/-}$ mouse, cone photoreceptors are its sole beneficiary, thus therapy in the *Rpe65*$^{-/-}$*::Rho*$^{-/-}$ mouse elicits more robust cone-mediated ERG responses. While more robust, cone-mediated responses in treated *Rpe65*$^{-/-}$*::Rho*$^{-/-}$ mice were still ~60% of their isogenic control (*Rho*$^{-/-}$ mice), a value similar to that seen when comparing ERG responses of treated *rd12* mice to WT controls. This is due to the fact that *Rho*$^{-/-}$mice exhibit 'supernormal' cone ERGs[26], a phenomenon that may also be attributed to cones in these mice existing as the sole beneficiary of 11-cis-retinal. These observations support delivery of clinical vector to central, cone-rich retinal regions of young LCA2 patients while attempting to minimize surgical manipulation of the macula. It is in these relatively cone-rich and rod-poor regions where chromophore "theft" is likely to be minimal and therefore where cones might benefit most from a vector-enhanced pool of 11-cis retinal.

In summary, our results show that AAV-mediated gene therapy prevents cone photoreceptor degeneration and preserves cone function in two genetically distinct models of *Rpe65*-LCA, the *rd12* and the *Rpe65*$^{-/-}$*::Rho*$^{-/-}$ mouse. Clearly however, vector must be administered prior to extensive cone degeneration. Additionally, we show that functional recovery in the *rd12* mouse, a model for human LCA2, is measurable within 4 days of treatment with a self complimentary, serotype 5 AAV vector expressing RPE65. With knowledge that Phase I LCA2 clinical trials presently show no short term safety concerns[11–15] as well as significant and quantifiable visual improvements[14, 15], this study supports the extension of human LCA2 trials into patients exhibiting less extensive retinal degeneration, particularly young patients who may have the most to gain from this therapy because they are more likely to retain significant central cone photoreceptor densities.

MATERIALS AND METHODS

Animals

C57BL/6J mice and the congenic inbred strain of *rd12* mice[38] were obtained from the Jackson Laboratory (Bar Harbor, ME). *Rpe65*$^{-/-}$::*Rho*$^{-/-}$ mice were generously provided by Baerbel Rohrer at the Medical University of South Carolina. All mice were bred and maintained in the University of Florida Health Science Center Animal Care Services Facilities under a 12hr/12hr light/dark cycle with less than 15 ft-c environmental illumination except where otherwise indicated. All experiments were approved by the local Institutional Animal Care and Use Committee and conducted in accordance with the ARVO Statement for the Use of Animals in Ophthalmic and Vision Research and NIH regulations.

scAAV5-smCBA-hRPE65 vector

Pseudotyped AAV5 capsid, self-complementary AAV vectors (scAAV) were used in this study as they have been show to be more efficient vectors for transduction of retina than standard, single stranded AAV vectors[20–23]. The scAAV5-smCBA-hRPE65 vector contains the small, hybrid CMV-chicken beta-actin (smCBA) promoter which has been shown to have identical transduction and tropism characteristics to full chimeric CMV-chicken beta-actin (CBA) promoter when targeted to the mouse retina[39]. The corresponding vector plasmid for scAAV5-smCBA-hRPE65 was constructed by replacing the humanized green

fluorescent protein (GFP) cDNA of sc-trs-smCBA-hGFP with the human RPE65 cDNA, via a Not I digest. Both contain flanking AAV serotype 2 inverted terminal repeats (ITR); one ITR has modifications required for packaging as a self complimentary AAV vector[40]. Vectors were manufactured and purified by previously described methods[41].Vector titer was determined by real time PCR and final aliquots were resuspended in balanced salt solution (Alcon Laboratories, Forth Worth TX, USA) containing 0.014% Tween 20.

Subretinal Injections

One μl of scAAV5-smCBA-hRPE65 vector (3.9×10^{10} delivered vector genomes) was injected subretinally into the left eyes of each P14 *rd12* mouse (n=5) and in the right eye three weeks later (P35). The same concentration of vector was injected subretinally into the right eyes of each P14 *Rpe65*$^{-/-}$::*Rho*$^{-/-}$ mouse (n=5). Subretinal injections were performed as previously described[41,42]. Further analysis was only carried out on mice which received comparable, successful injections (>60% retinal detachment, and minimal complications). We only chose *rd12* mice, in which both eyes showed similar retinal detachments and *Rpe65*$^{-/-}$*::Rho*$^{-/-}$ mice with equally comparable unilateral detachments following subretinal injections for further analysis. It is well established that the area of retinal detachment corresponds to area of viral transduction[14,44].

Electroretinographic analysis

ERGs of *rd12* mice were recorded using protocols modified from previous studies[20,45,46]. Briefly, mice were dark adapted overnight and anesthetized with a mixture of ketamine (75 mg/kg intramuscularly) and xylazine (13.6 mg/kg intramuscularly). Pupils were dilated with 1% tropicamide and 2.5% phenylephrine hydrochloride, and a heating pad was used to keep the body temperature at 38 C. The corneal electrode was a gold wire loop; a reference electrode was placed on the forehead and a ground electrode was applied subcutaneously near the tail. Signals were amplified at 10,000 gain and bandpass filtered between 0.1 and 1000 Hz. The signals were digitized at 5.12 kHz for conventional ERG with a data acquisition device (National Instrument, Austin, TX). To increase the signal noise ratio, 3~6 signals were averaged for conventional dark-adapted ERG; whereas 12~16 signals were averaged for light-adapted responses using a custom-compiled program (LabView 7.1, National Instrument, Austin, TX).

Ganzfeld illumination employed a Grass PS22 Xenon visual stimulator (Grass Instrument Inc. West Warwick, RI). The light flash had duration of 10 μs, and the maximum intensity was 0.65 log cd-s/m^2. A timer (Uniblitz, Rochester, NY) was used to control the frequency of the flash. In dark-adapted ERG recordings, the interstimulus interval (ISI) was at least 12 seconds for low intensities and more than 30 seconds for high intensities. For light-adapted ERG recordings, a background light of 30 cd/m^2 was applied to suppress rod responses. The stimulus light intensity was attenuated with neutral density filters (Kodak, Rochester, NY) and luminance was calibrated with an IL-1700 integrating radiometer/photometer (International Light, Newburyport, MA).

ERGs of *Rpe65*$^{-/-}$::*Rho*$^{-/-}$ mice and *rd12* mice 4 days after P14 treatment were recorded using a UTAS Visual Diagnostic System with a Big Shot Ganzfeld (LKC Technologies, Gaithersburg, MD). Mice were dark adapted, anesthetized and dilated according to methods used for *rd12* mice. Gold wire loop electrodes were placed on each cornea and a reference electrode placed near the nose. Dark-adapted-ERGs of the *rd12* mouse 4 days after P14 treatment were applied at 0.4 log cd-s/m^2. All photopic measurements were taken in the presence of 30 cd/m^2 background light. Signal to noise ratios were increased by averaging 50 signals at each light intensity (ranging from 0.1–1.4 log cd-s/m^2) using LKC software, EM for Windows Version 7.0 (LKC Technologies, Gaithersburg, MD). Ganzfeld

illumination with white light was applied for a duration of 2.4 ms. The interstimulus interval was 0.4 seconds at all intensities. ERG signals were analyzed with the LKC EM for Windows software. B-wave amplitudes were defined as the difference between the trough and peak of each waveform. Photopic b-wave maximum amplitudes (those generated at the 1.4 log cd-s/m^2 intensity) of all *Rpe65*$^{-/-}$::*Rho*$^{-/-}$ mice (both treated and untreated eyes) were averaged and used to generate standard errors. This data was imported into Sigma Plot for final graphical presentation.

ERG data are presented as mean ± standard deviation (mean ± SD). Statistical significance was examined with ANOVA. Pair wise comparisons between groups for the ERG were performed by the Bonferroni post hoc test. A *P* value of less than 0.05 was considered as significant.

Optomotor testing

Photopic and scotopic visual acuities and contrast sensitivities of treated and untreated mouse eyes were measured using a two-alternative forced choice paradigm as described previously[47,48] with minor modifications. To separately test the sensitivity of each eye from the same animal we took advantage of the fact that mouse vision has minimal binocular overlap and that the left eye is more sensitive to clockwise rotation and the right to counter-clockwise rotation[49]. Thus in our "randomize-separate" optomotor protocol, acuities or contrast sensitivities for each eye were determined separately, with correct detection of patterns rotating in the clockwise direction vision being detected by the left eye and correct responses in the counterclockwise direction being driven primarily by visual signals originating from the right eye. Thresholds for each eye were determined simultaneously via stepwise functions for correct responses in both the clockwise and counter-clockwise direction. Acuity was defined the highest spatial frequency (100% contrast) yielding a threshold response, and contrast sensitivity was defined as 100 divided by the lowest percent contrast (pattern of 0.256 cycles/degree) yielding a threshold response. For both photopic and scotopic acuity, the initial stimulus was a 0.200 cycles/degree sinusoidal pattern with a fixed 100% contrast. For photopic contrast sensitivity measurements, the initial pattern was presented at 100% contrast, with a fixed spatial frequency of 0.256 cycles/degree. For scotopic contrast sensitivity measurements, the spatial frequency was fixed at 0.031 cycles/degree, a spatial frequency tuned for rod vision[47]. All patterns were presented at a speed of 12 degrees per second. Photopic vision was measured at a mean luminance of 70 cd/m^2. For scotopic measurements, mice were dark-adapted overnight and light levels were attenuated to 3.5×10^{-5} cd/m^2 through the use of neutral density filters. Visual acuities and contrast sensitivities were measured for both eyes of each mouse four to six times over a period of 1–2 weeks. Wild type control animals were 6 months old at testing time (n=4), and P14 treated animals were at least 6 months old (n=4). Untreated eyes from 6-month *rd12* mice (n=3), opposite from those that received treatment at P35 (n=3), are presented as the untreated group in bar graphs. Unpaired t-tests were carried out on acuity and percent contrast values to determine significance of results.

Tissue preparation and immunohistochemistry

Eyes of P14- and P35- treated *rd12* mice were enucleated at 6 months and 5 months of age, respectively. For comparison, eyes of untreated *rd12* mice were enucleated at 2 weeks, 5 weeks and 5 months of age. Eyes of P14-treated and untreated *Rpe65*$^{-/-}$::*Rho*$^{-/-}$ mice were enucleated at P42. Eyes of control *C57BL/6J* were enucleated at 2 weeks of age. Retinal wholemounts were prepared according to previously described methods [50,51]. Briefly, immediately following sacrifice, the limbus of injected and uninjected eyes was marked at "12 o'clock" with a burned needle which facilitated orientation. The eyes were then enucleated and fixed in 4% paraformaldehyde. Cornea, lens, vitreous and retinal pigment

epithelium were removed from each eye without disturbing the retina. Fixed retinal wholemounts were washed in 1X PBS and incubated in blocking solution (2% normal goat serum, 0.3% Triton X-100 in 1% BSA in PBS) for 30–60 minutes at room temperature. Samples were washed one time briefly with 0.3% Triton X-100 and 1% BSA in PBS and then incubated 24–48 hours in the dark at 4° with either S-cone opsin and M-cone opsin primary antibodies (Santa Cruz Biotechnology, Santa Cruz, CA) diluted 1:500 in 0.1% Triton X-100 and 1% BSA in PBS. Following incubation in primary antibodies, wholemounts were rinsed with PBS and incubated in the dark at 4° overnight in IgG secondary antibodies tagged with either Alexa-594 or Alexa-488 fluorophore (Molecular Probes, Eugene, OR) diluted 1:500 in PBS. Wholemounts were rinsed with 1X PBS and then incubated in FITC-conjugated peanut agglutinin (PNA) diluted 1:100 in 10% normal goat serum at 4° overnight, in the dark. After a final rinse with 1X PBS, wholemounts were oriented on slides with the superior (dorsal) portion of the retina positioned at 12:00. Samples were mounted in fluorescent mounting media (DAKO, Carpinteria, CA) and analyzed with a Zeiss CD25 microscope fitted with Axiovision Rel. 4.6 software. All fluorescent images were acquired using identical exposure settings.

Images were saved as TIFF files and analyzed using Image J software. Cone cell densities were determined by counting cells labeled with secondary fluorophores directed against either PNA, MWL or SWL antibodies in the central, dorsal temporal, ventral temporal, dorsal nasal and ventral nasal retinal quadrants of *rd12* or *Rpe65*$^{-/-}$*::Rho*$^{-/-}$ mice. These values were obtained using high magnification images (10X) of the wholemounts shown in Figures 1,4, 5 and 7 as well as P14 WT retinas stained for MWL and SWL cone opsin (10X images not shown). Five squares (500μm^2) were placed over identical areas of each central retina and four respective quadrants (total squares per retinal wholemount = 25). The squares were placed at a minimum of 6000 μm from the optic disc in all four peripheral quadrants. Cone photoreceptors were counted in each respective retinal area, values were averaged and standard deviations calculated. The standard t-test was used to calculate p-values between desired samples. Significant difference was defined as a p-value < 0.05. Data is presented in Table 2 and Supplemental Tables 1, 2a, 2b, 3a, and 3b. As an additional measure of cone cell preservation, we also performed a similar analysis using measurements of fluorescence intensity. The results were the same (data not shown). Supplementary information is available at Gene Therapy's website.

Supplementary Material

Refer to Web version on PubMed Central for supplementary material.

Acknowledgments

We thank Vince Chiodo and Thomas Doyle at the University of Florida and Keqing Zhang at the University of Missouri for their technical support. We also acknowledge NIH grants EY018331, EY13729, EY11123, NS36302, EY08571, EY07758, EY014046, EY06360, EY017246(DE), EY00067 (RB) and grants from the Macular Vision Research Foundation, Foundation Fighting Blindness, Fight for Sight (DE), Lions of Central NY, NASA (RB), Juvenile Diabetes Research Foundation and Research to Prevent Blindness, Inc. for partial support of this work. W.W.H. and the University of Florida have a financial interest in the use of AAV therapies, and own equity in a company (AGTC Inc.) that might, in the future, commercialize some aspects of this work.

References

1. Marlhens F, Bareil C, Griffoin JM, Zrenner E, Amalric P, Eliaou C, et al. Mutations in RPE65 cause Leber's congenital amaurosis. Nat Genet 1997;17:139–41. [PubMed: 9326927]
2. Rohrer B, Lohr HR, Humphries P, Redmond TM, Seeliger MW, Crouch RK. Cone opsin mislocalization in Rpe65−/− mice: a defect that can be corrected by 11-cis retinal. Invest Ophthalmol Vis Sci 2005;46:3876–82. [PubMed: 16186377]

3. Zhang H, Fan J, Li S, Karan S, Rohrer B, Palczewski K, et al. Trafficking of membrane-associated proteins to cone photoreceptor outer segments requires the chromophore 11-cis-retinal. J Neurosci 2008;28:4008–14. [PubMed: 18400900]
4. Feathers KL, Lyubarsky AL, Khan NW, Teofilo K, Swaroop A, Williams DS, et al. Nrl-knockout mice deficient in Rpe65 fail to synthesize 11-cis retinal and cone outer segments. Invest Ophthalmol Vis Sci 2008;49:1126–35. [PubMed: 18326740]
5. Jacobson SG, Aleman TS, Cideciyan AV, Heon E, Golczak M, Beltran WA, et al. Human cone photoreceptor dependence on RPE65 isomerase. Proc Natl Acad Sci U S A 2007;104:15123–8. [PubMed: 17848510]
6. Jacobson SG, Cideciyan AV, Aleman TS, Sumaroka A, Windsor EA, Schwartz SB, et al. Photoreceptor layer topography in children with leber congenital amaurosis caused by RPE65 mutations. Invest Ophthalmol Vis Sci 2008;49:4573–7. [PubMed: 18539930]
7. Mata NL, Ruiz A, Radu RA, Bui TV, Travis GH. Chicken retinas contain a retinoid isomerase activity that catalyzes the direct conversion of all-trans-retinol to 11-cis-retinol. Biochemistry 2005;44:11715–21. [PubMed: 16128572]
8. Muniz A, Villazana-Espinoza ET, Hatch AL, Trevino SG, Allen DM, Tsin AT. A novel cone visual cycle in the cone-dominated retina. Exp Eye Res 2007;85:175–84. [PubMed: 17618621]
9. Schonthaler HB, Lampert JM, Isken A, Rinner O, Mader A, Gesemann M, et al. Evidence for RPE65-independent vision in the cone-dominated zebrafish retina. Eur J Neurosci 2007;26:1940–9. [PubMed: 17868371]
10. Wang JS, Estevez ME, Cornwall MC, Kefalov VJ. Intra-retinal visual cycle required for rapid and complete cone dark adaptation. Nat Neurosci 2009;12:295–302. [PubMed: 19182795]
11. Bainbridge JW, Smith AJ, Barker SS, Robbie S, Henderson R, Balaggan K, et al. Effect of gene therapy on visual function in Leber's congenital amaurosis. N Engl J Med 2008;358:2231–9. [PubMed: 18441371]
12. Maguire AM, Simonelli F, Pierce EA, Pugh EN Jr, Mingozzi F, Bennicelli J, et al. Safety and efficacy of gene transfer for Leber's congenital amaurosis. N Engl J Med 2008;358:2240–8. [PubMed: 18441370]
13. Hauswirth W, Aleman TS, Kaushal S, Cideciyan AV, Schwartz SB, Wang L, et al. Treatment of leber congenital amaurosis due to RPE65 mutations by ocular subretinal injection of adeno-associated virus gene vector: short-term results of a phase I trial. Hum Gene Ther 2008;19:979–90. [PubMed: 18774912]
14. Cideciyan AV, Aleman TS, Boye SL, Schwartz SB, Kaushal S, Roman AJ, et al. Human gene therapy for RPE65 isomerase deficiency activates the retinoid cycle of vision but with slow rod kinetics. Proc Natl Acad Sci U S A 2008;105:15112–7. [PubMed: 18809924]
15. Cideciyan AV, Hauswirth WW, Aleman TS, Kaushal S, Schwartz SB, Boye, et al. Vision One Year after Gene Therapy for Leber Congenital Amaurosis. New Eng J Med 2009;361:725–727. [PubMed: 19675341]
16. Cronin T, Leveillard T, Sahel JA. Retinal degenerations: from cell signaling to cell therapy: preclinical and clinical issues. Curr Gene Ther 2007;7:121–9. [PubMed: 17430131]
17. Samardzija M, Tanimoto N, Kostic C, Beck S, Oberhauser V, Joly S, et al. In conditions of limited chromophore supply rods entrap 11-cis-retinal leading to loss of cone function and death. Hum Mol Genet 2009;18:1266–75. [PubMed: 19147682]
18. Carroll J, Choi SS, Williams DR. In vivo imaging of the photoreceptor mosaic of a rod monochromat. Vision Res 2008;48:2564–8. [PubMed: 18499214]
19. Seeliger MW, Grimm C, Ståhlberg F, Friedburg C, Jaissle G, Zrenner E, et al. New views on RPE65 deficiency: the rod system is the source of vision in a mouse model of Leber congenital amaurosis. Nat Genet 2001;29:70–4. [PubMed: 11528395]
20. Hauswirth WW, Petrs-Silva H, Min S-H, Boye SE, Liu JM, Mani S, et al. Self-Complementary AAV Vectors Promote Fast and Efficient Transduction of Mouse Retina. Invest Ophthalmol Vis Sci 2006;47 ARVO E-Abstract 839.
21. Yokoi K, Kachi S, Zhang HS, Gregory PD, Spratt SK, Samulski RJ, et al. Ocular gene transfer with self-complementary AAV vectors. Invest Ophthalmol Vis Sci 2007;48:3324–8. [PubMed: 17591905]

22. Natkunarajah M, Trittibach P, McIntosh J, Duran Y, Barker SE, Smith AJ, et al. Assessment of ocular transduction using single-stranded and self-complementary recombinant adeno-associated virus serotype 2/8. Gene Ther 2008;15:463–7. [PubMed: 18004402]
23. Li Q, Kong F, Li X, Dai X, Liu X, Zheng Q, et al. Gene therapy following subretinal AAV5 vector delivery is not affected by a previous intravitreal AAV5 vector administration in the partner eye. Mol Vis 2009;15:267–75. [PubMed: 19190735]
24. Léveillard T, Mohand-Saïd S, Lorentz O, Hicks D, Fintz AC, Clérin E, et al. Identification and characterization of rod-derived cone viability factor. Nat Genet 2004;36:755–9. [PubMed: 15220920]
25. Sahel JA. Saving cone cells in hereditary rod diseases: a possible role for rod-derived cone viability factor (RdCVF) therapy. Retina 2005;25:S38–S39. [PubMed: 16374327]
26. Jaissle GB, May CA, Reinhard J, Kohler K, Fauser S, Lutjen-Drecoll E, et al. Evaluation of the rhodopsin knockout mouse as a model of pure cone function. Invest Ophthalmol Vis Sci 2001;42:506–13. [PubMed: 11157890]
27. Redmond TM, Yu S, Lee E, Bok D, Hamasaki D, Chen N, et al. Rpe65 is necessary for production of 11-cis-vitamin A in the retinal visual cycle. Nat Genet 1998;20:344–51. [PubMed: 9843205]
28. Znoiko SL, Rohrer B, Lu K, Lohr HR, Crouch RK, Ma JX. Downregulation of cone-specific gene expression and degeneration of cone photoreceptors in the Rpe65−/− mouse at early ages. Invest Ophthalmol Vis Sci 2005;46:1473–9. [PubMed: 15790918]
29. Bemelmans AP, Kostic C, Crippa SV, Hauswirth WW, Lem J, Munier FL, et al. Lentiviral gene transfer of RPE65 rescues survival and function of cones in a mouse model of Leber congenital amaurosis. PLoS Med 2006;3:e347. [PubMed: 17032058]
30. Chen Y, Moiseyev G, Takahashi Y, Ma JX. RPE65 gene delivery restores isomerohydrolase activity and prevents early cone loss in Rpe65−/− mice. Invest Ophthalmol Vis Sci 2006;47:1177–84. [PubMed: 16505056]
31. Cramer W, Stowell RE. Carcinogenesis in the mouse's skin by the infrequent application at long intervals of mehtylcholanthrene. Cancer Research 1941;1:849–52.
32. Humphries MM, Rancourt D, Farrar GJ, Kenna P, Hazel M, Bush RA, et al. Retinopathy induced in mice by targeted disruption of the rhodopsin gene. Nat Genet 1997;15:216–9. [PubMed: 9020854]
33. Lem J, Krasnoperova NV, Calvert PD, Kosaras B, Cameron DA, Nicolò M, et al. Morphological, physiological, and biochemical changes in rhodopsin knockout mice. Proc Natl Acad Sci U S A 1999;96:736–41. [PubMed: 9892703]
34. Hewitt AT, Lindsey JD, Carbott D, Adler R. Photoreceptor survival-promoting activity in interphotoreceptor matrix preparations: characterization and partial purification. Exp Eye Res 1990;50:79–88. [PubMed: 2307198]
35. Bird AC. Investigation of disease mechanisms in retinitis pigmentosa. Ophthalmic Paediatr Genet 1992;13:57–66. [PubMed: 1495768]
36. Petters RM, Alexander CA, Wells KD, Collins EB, Sommer JR, Blanton MR, et al. Genetically engineered large animal model for studying cone photoreceptor survival and degeneration in retinitis pigmentosa. Nat Biotechnol 1997;15:965–70. [PubMed: 9335046]
37. Ostrer H, Pullarkat RK, Kazmi MA. Glycosylation and palmitoylation are not required for the formation of the X-linked cone opsin visual pigments. Mol Vis 1998;4:28. [PubMed: 9852167]
38. Pang J, Chang B, Hawes NL, Hurd RE, Davisson MT, Li J, et al. Retinal Degeneration 12 (rd12): A new, spontaneously arising mouse model for human Leber congenital amaurosis (LCA). Mol Vis 2005;11:152–62. [PubMed: 15765048]
39. Haire SE, Pang J, Boye SL, Sokal I, Craft CM, Palczewski K, et al. Light-driven cone arrestin translocation in cones of postnatal guanylate cyclase-1 knockout mouse retina treated with AAV-GC1. Invest Ophthalmol Vis Sci 2006;47:3745–53. [PubMed: 16936082]
40. McCarty DM, Fu H, Monahan PE, Toulson CE, Naik P, Samulski RJ. Adeno-associated virus terminal repeat (TR) mutant generates self-complementary vectors to overcome the rate-limiting step to transduction in vivo. Gene Ther 2003;10:2112–8. [PubMed: 14625565]
41. Hauswirth WW, Lewin AS, Zolotukhin S, Muzyczka N. Production and purification of recombinant adeno-associated virus. Methods Enzymol 2000;316:743–61. [PubMed: 10800712]

42. Pang J, Chang B, Kumar A, Nusinowitz S, Noorwez SM, Li J, et al. Gene therapy restores vision-dependent behavior as well as retinal structure and function in a mouse model of RPE65 Leber congential amaurosis. Mol Ther 2006;13:565–72. [PubMed: 16223604]
43. Pang J, Boye SL, Kumar A, Dinculescu A, Deng W, Li J, et al. AAV-mediated gene therapy delays retinal degeneration in the *rd10* mouse containing a recessive PDEβ mutation. Invest Ophthalmol Vis Sci 2008;49 (10):4278–4283. [PubMed: 18586879]
44. Timmers AM, Zhang H, Squitieri A, Bonzalez-Pola C. Subretinal injections in rodent eyes: effects on electrophysiology and histology of rat retina. Mol Vis 2001;7:131–7. [PubMed: 11435999]
45. Lei B, Yao G, Zhang K, Hofeldt KJ, Chang B. Study of rod- and cone-driven oscillatory potentials in mice. Invest Ophthalmol Vis Sci 2006;47:2732–38. [PubMed: 16723493]
46. Lei B, Zhang K, Yue Y, Ghosh A, Duan D. Adeno-associated virus serotype-9 efficiently transduces the photoreceptor terminals. Mol Vis 2009;17:1374–82. [PubMed: 19626133]
47. Umino Y, Solessio E, Barlow RB. Speed, spatial, and temporal tuning of rod and cone vision in mouse. J Neurosci 2008;28:189–98. [PubMed: 18171936]
48. Alexander JJ, Umino Y, Everhart D, Chang B, Min SH, Li Q, et al. Restoration of cone vision in a mouse model of achromatopsia. Nat Med 2007;13:685–7. [PubMed: 17515894]
49. Douglas RM, Alam NM, Silver BD, McGill TJ, Tschetter WW, Prusky GT. Independent visual threshold measurements in the two eyes of freely moving rats and mice using a virtual-reality optokinetic system. Vis Neuro 2005;22:677–684.
50. Pang J, Cheng M, Haire SE, Barker E, Planelles V, Blanks JC. Efficiency of lentiviral transduction during development in normal and rd mice. Mol Vision 2006;12:756–767.
51. Pang J, Lauramore A, Deng W, Li Q, Doyle T, Chiodo V, et al. Analysis of in vivo and in vitro AAV vector transduction in neonatal mouse retina: effects of serotype and site of administration. Vision Res 2008;48:377–385. [PubMed: 17950399]

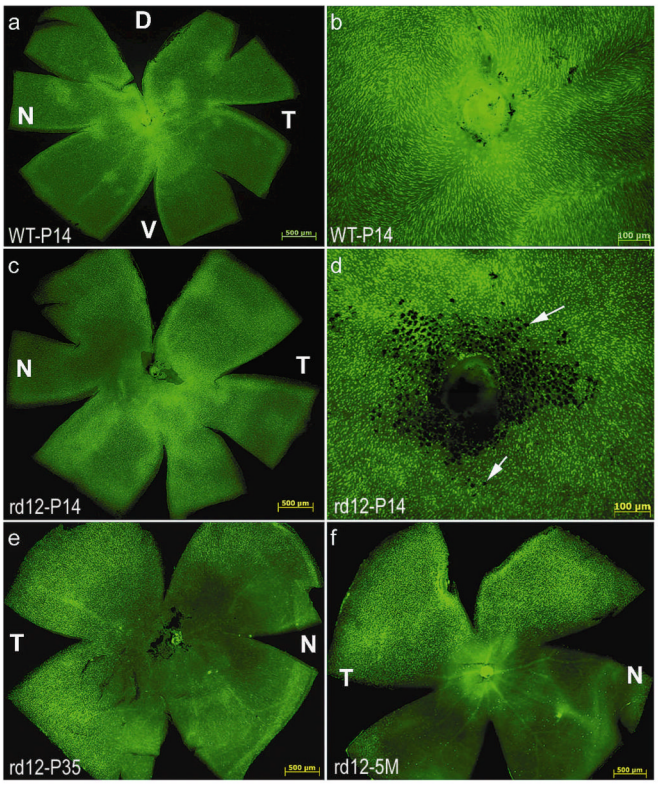

Figure 1. Temporal analysis of cone photoreceptor densities in *rd12* and wild type mouse retinas

FITC-labeled Peanut Agglutinin (PNA) staining revealed that cone photoreceptors were abundant in the central and peripheral regions of the untreated, P14 *rd12* mouse retina (**c, d**), a pattern similar to that seen in the P14, wild type mouse retina (**a, b**). Cones degenerate in the *rd12* retina by 5 weeks of age (**e**), remaining only in the dorsal and temporal regions through at least 5 months (**f**). Arrows: fragments of RPE cells. D: dorsal; V: ventral; T: temporal; N: nasal.

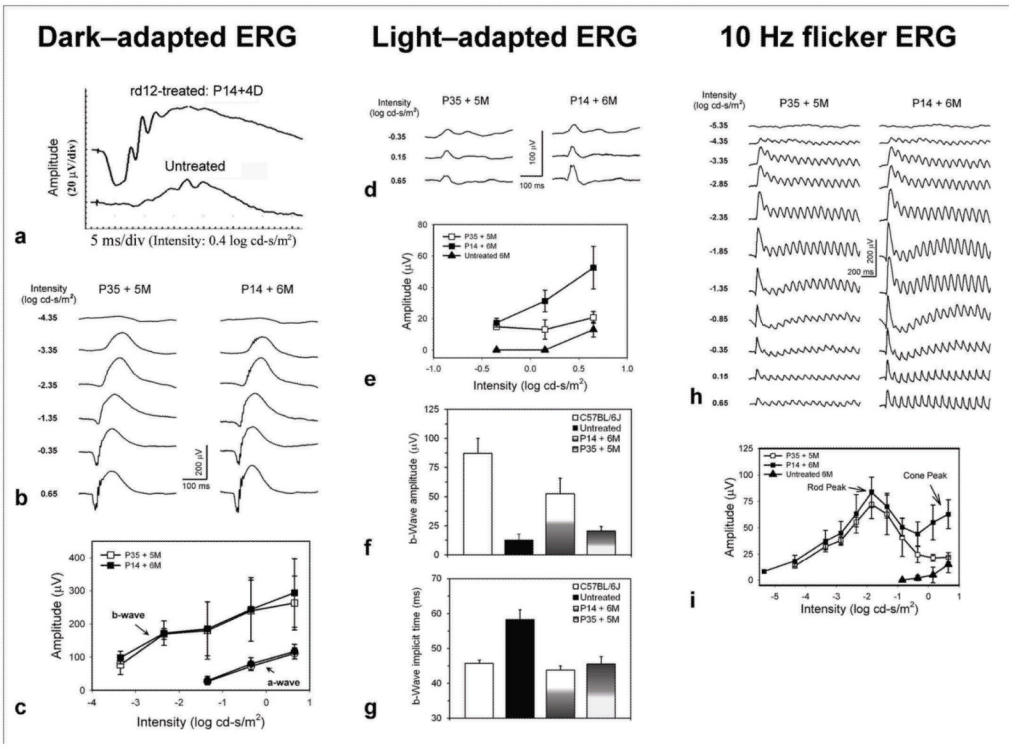

Figure 2. Comparison of rod- and cone-driven functions in *rd12* mice after early P14- or late P35-subretinal deliveries of a scAAV5-smCBA-hRPE65 vector

The left, middle and right columns show dark-adapted, light-adapted and 10 Hz flicker ERGs respectively. P14 treatment resulted in functional rescue to rod system as early as 4 days post injection (**a**). Representative dark-adapted ERGs recorded at 6 or 5 months after P14 (left eye) and P35 (right eye) treatment showed robust restoration of the rod system functions (**b** and **c**), as indicated by significant increases of both a- and b-wave amplitudes (**c**) relative to untreated controls which had minimal responses. For the light-adapted ERG, P14-treatment significantly improved the b-wave amplitudes to a level about 60% of normal uninjected controls (**d, e** and **f**); whereas P35-treatment did not result in significant b-wave amplitude increase compared to untreated *rd12* mice (**f**). Light-adapted ERG showed that both P14- and P35-treatments significantly reduced the delayed b-wave implicit time to normal levels (**g**). Both representative (**h**) and statistical (**i**) data from 10 Hz flicker ERGs.

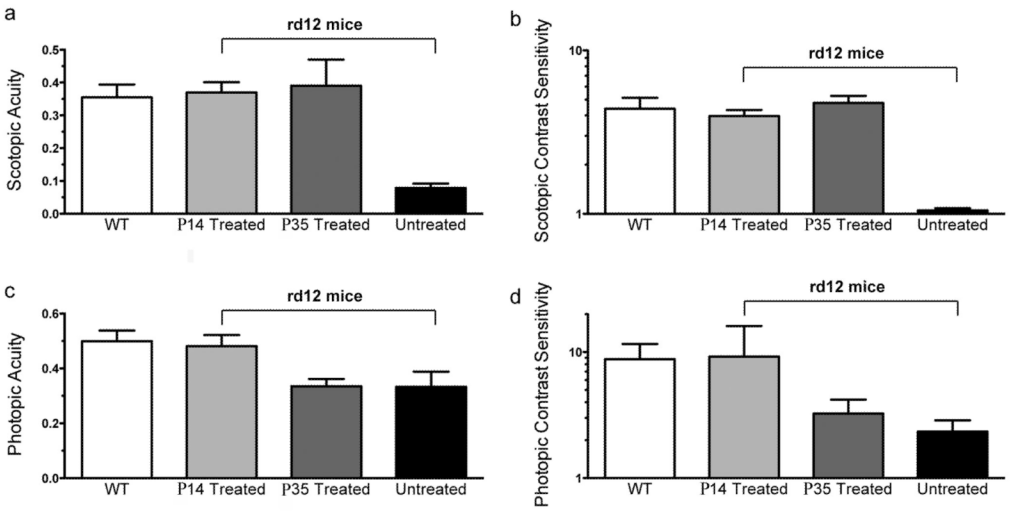

Figure 3. scAAV-RPE65 treatment restores photopic vision in *rd12* mice treated at P14, and scotopic vision in *rd12* mice treated at P14 or P35

Under scotopic conditions, treatment with AAV-RPE65 at P14 (light grey bar, n=4 eyes, and at P35 (dark grey bar, n=3 eyes) leads to acuities (**a**) and contrast sensitivities (**b**) comparable to uninjected C57BL/6 mice (white bars, n=4 eyes). Untreated *rd12* eyes (black bars, n=3) perform significantly poorer in tests of both scotopic acuity (**a**) and scotopic contrast sensitivity (**b**) than those from C57 or treated *rd12* eyes. The level of vision in these untreated eyes is equivalent to no visual function. Under photopic conditions, (**c**) *rd12* mouse eyes treated with AAV-RPE65 at P14 (light grey bar, n=4) have significantly better acuity than untreated *rd12* control eyes (black bar, n=3) and maintain photopic acuity comparable to wild type C57BL/6J eyes (white bar, n=4), while eyes treated at P35 (dark grey bar, n=3 eyes) show no significant change from their untreated *rd12* counterparts (black bar, n=3 eyes). (**d**) As with photopic contrast sensitivity, *rd12* eyes treated at P14 (light grey bar, n=4 eyes), but not those treated at P35 (dark grey bar, n=3 eyes) exhibit photopic contrast sensitivity near wild type C57BL/6J levels (white bar, n=4 eyes).

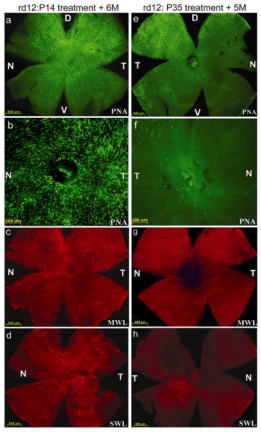

Figure 4. Retinalwhole mounts of *rd12* mice treated at P14 (left column) or P35 (right column) with scAAV5-hRPE65 and stained with PNA, MWL-cone opsin antibody or SWL-cone opsin antibody

PNA staining revealed that cones were abundant in the peripheral (**a**) and central (**b**) regions of the P14 treated *rd12* retina. P14 treated cones were positive for both MWL cone opsin (**c**) and SWL cone opsin (**d**). Cone specific PNA staining after P35 treatment was reduced centrally (**f**) and was restricted to dorsal and temporal retina (**e**), a pattern similar to that seen in the P35 untreated, *rd12* retina. P35 treated cones contained MWL cone opsin (**g**), but lacked detectable SWL cone opsin (**h**). D: dorsal; V: ventral; T: temporal; N: nasal.

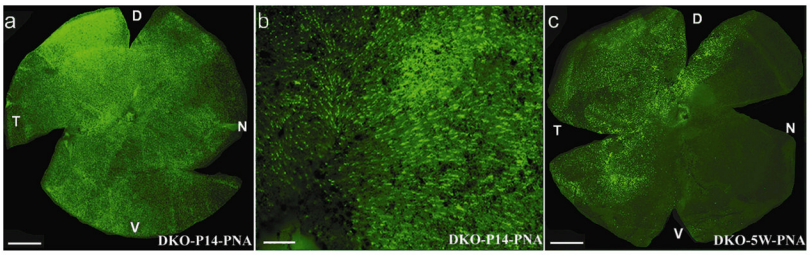

Figure 5. Temporal analysis of cone photoreceptor densities in the *Rpe65*$^{-/-}$*::Rho*$^{-/-}$ mouse retina

PNA staining (**a, b)** revealed that cone photoreceptors were abundant in the central and peripheral regions of the untreated, P14 *Rpe65*$^{-/-}$*::Rho*$^{-/-}$ mouse retina, a pattern similar to that seen in the P14, wild type mouse retina (see Fig 1a, b). Cones degenerate in the *Rpe65*$^{-/-}$*::Rho*$^{-/-}$retina by 5 weeks of age (**c**), remaining only in the dorsal and temporal retina. D: dorsal; V: ventral; T: temporal; N: nasal. DKO: *Rpe65*$^{-/-}$*::Rho*$^{-/-}$ double knockout mouse. Scale bars (**a, c**) = 500 μM. Scale bar (**b**) = 100 μM.

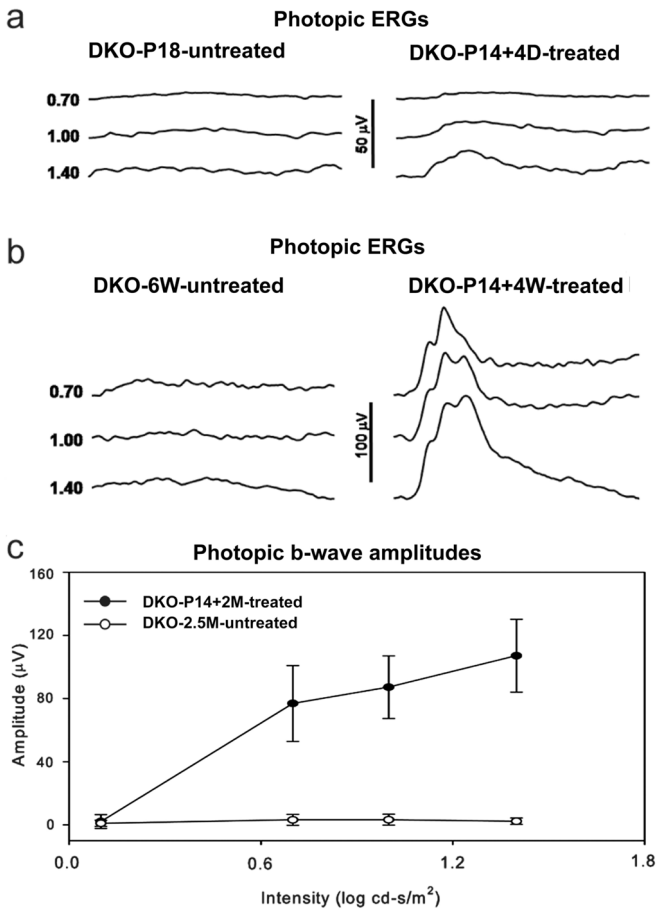

Figure 6. Photopic electroretinogram in *Rpe65*$^{-/-}$*::Rho*$^{-/-}$mice

Cone responses were detectable within 4 days after vector treatment (**a**). These responses increased in amplitude (**b**) and remained stable until at least P42, the latest time point tested. Treated eyes of *Rpe65*$^{-/-}$*::Rho*$^{-/-}$mice (n=5) had significantly higher photopic b-wave amplitudes than untreated eyes (**c**). DKO: *Rpe65*$^{-/-}$*::Rho*$^{-/-}$ double knockout mouse.

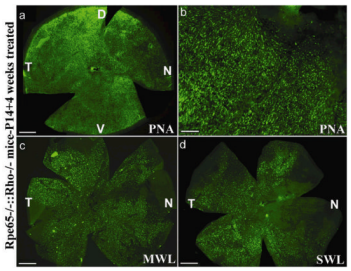

Figure 7. Retinal whole mounts of *Rpe65*$^{-/-}$*::Rho*$^{-/-}$ mice 4 weeks after vector treatment at P14 and stained with PNA, MWL-cone opsin antibody or SWL-cone opsin antibody

PNA staining revealed that cones were abundant in the peripheral (**a**) and central (**b**) regions of a P14 treated *Rpe65*$^{-/-}$*::Rho*$^{-/-}$ retina. These cones were positive for both MWL cone opsin (**c**) and SWL cone opsin (**d**). D: dorsal; V: ventral; T: temporal; N: nasal. Scale bars (a, c, d) = 500 μM. Scale bar (**b**) = 100 μM.

Table 1

Statistical comparison of the scotopic and photopic visual function of wild type, P14 vector treated, P35 vector treated, and untreated rd12 mouse eyes as measured by optomotor behavior

Under scotopic conditions, P14 and P35 treatment produces acuity and contrast sensitivity similar to wild type animals and wild type, P14-treated and P35-treated eyes all have significantly better acuity and contrast sensitivity than untreated rd12 eyes. Under photopic conditions, only P14 treated eyes are not significantly different from wild type eyes; P35 treatment eyes did not differ significantly from rd12 untreated eyes for both photopic acuity and contrast sensitivity. Each mouse was tested for 4–6 trials per condition. Data from each animal (n=3–4) were then averaged to obtain the means for each condition. The standard deviation listed is the standard deviation of the individual mouse means.

Scotopic Acuity	**WT**	**p14**	**p35**	**Untreated**	WT vs p14	P = 0.5751	Not significant
Number of mice	4	4	3	3	WT vs p35	P = 0.4713	Not significant
Mean	0.355	0.3698	0.3899	0.07858	WT vs Untreated	P< 0.0001	***
Standard Deviation	0.03876	0.03125	0.07975	0.01313	Untreated vs p14	P< 0.0001	***
					Untreated vs p35	P = 0.0026	**
Scotopic Contrast Sensitivity	**WT**	**p14**	**p35**	**Untreated**	WT vs p14	P = 0.3924	Not significant
Number of mice	4	4	3	3	WT vs p35	P = 0.4486	Not significant
Mean	4.398	3.967	4.775	1.051	WT vs Untreated	P< 0.0001	***
Standard Deviation	0.739	0.3479	0.4946	0.03153	Untreated vs p14	P< 0.0001	***
					Untreated vs p35	P< 0.0001	***
Photopic Acuity	**WT**	**p14**	**p35**	**Untreated**	WT vs p14	P = 0.5467	Not significant
Number of mice	4	4	3	3	WT vs p35	P = 0.0016	**
Mean	0.4993	0.4813	0.3346	0.3329	WT vs Untreated	P = 0.0053	**
Standard Deviation	0.03886	0.04046	0.02716	0.0555	Untreated vs pi4	P = 0.0091	**
					Untreated vs p35	P = 0.9644	Not significant
Photopic Contrast Sensitivity	**WT**	**p14**	**p35**	**Untreated**	WT vs p14	P = 0.4718	Not significant
Number of mice	4	4	3	3	WT vs p35	P = 0.0094	**
Mean	8.793	9.19	3.25	2.339	WT vs Untreated	P = 0.0031	**
Standard Deviation	2.79	6.925	0.9493	0.5343	Untreated vs p14	P = 0.022	*
					Untreated vs p35	P = 0.2301	Not significant

P-values were calculated using an unpaired two-tailed t test.

*** $p < 0.001$,

** $p < 0.01$,

* $p < 0.05$.

Table 2

Summary of comparisons of cone cell quantifications in treated and untreated *rd12*, *Rpe65*$^{-/-}$*::Rho*$^{-/-}$ or wild type retinas as measured by PNA, MWL or SWL cone opsin immunostaining

Cone photoreceptors were counted in the central (C), dorsal temporal (DT), ventral temporal (VT), dorsal nasal (DN) and ventral nasal (VN) quadrants of each retina. Values were calculated and averaged in five areas (500 μm^2) per quadrant. A standard t-test was used to calculate p-values between desired samples. Significant difference was defined as a p value < 0.05.

	C	DT	VT	DN	VN
Figure 1					
P14 WT vs. P14 rd12 (PNA)					
P14 WT vs. 5 weeks rd12 (PNA)	*		*	*	*
P14 WT vs. 5 months rd12 (PNA)	*		*	*	*
P14 rd12 vs. 5 weeks rd12 (PNA)	*		*	*	*
P14 rd12 vs. 5 months rd12 (PNA)	*		*	*	*
5 weeks rd12 vs. 5 months rd12 (PNA)			*	*	
Figure 4					
P14 WT vs. P14-treated rd12 (PNA)					
P14 WT vs. P35-treated rd12 (PNA)	*		*	*	*
P14 WT vs. P14-treated rd12 (MWL)	*		*		*
P14 WT vs. P14-treated rd12 (SWL)	*				*
P14 WT vs. P35-treated rd12 (MWL)	*		*		*
P14 WT vs. P35-treated rd12 (SWL)	*	*	*	*	*
P14-treated rd12 vs. P35-treated rd12 (PNA)	*		*	*	*
P14-treated rd12 vs. P35-treated rd12 (MWL)					*
P14-treated rd12 vs. P35-treated rd12 (SWL)	*	*	*	*	*
P35-treated rd12 vs. 5 months rd12 (PNA)					
Figures 5 and 7					
P14 DKO vs. P14 WT (PNA)					
P14 DKO vs. 5 weeks DKO (PNA)	*		*	*	*
P14 WT vs. 5 weeks DKO (PNA)	*		*	*	*
P14-treated DKO vs. P14 WT (PNA)					
P14-treated DKO vs. P14 DKO (PNA)					
P14-treated DKO vs. P14 WT (MWL)				*	

Gene Ther. Author manuscript; available in PMC 2011 July 1.

	C	DT	VT	DN	VN
P14-treated DKO vs. P14 WT (SWL)	*				*